

## ARTICLES

## Inclusive scattering of polarized electrons on polarized $^3\text{He}$ : Effects of final state interaction and the magnetic form factor of the neutron

S. Ishikawa

*Department of Physics, Hosei University, Fujimi 2-17-1, Chiyoda, Tokyo 102, Japan*

J. Golak and H. Witała

*Institute of Physics, Jagellonian University, PL-30059 Cracow, Poland*

H. Kamada,\* W. Glöckle, and D. Hüber†

*Institut für Theoretische Physik II, Ruhr-Universität Bochum, D-44780 Bochum, Germany*

(Received 31 July 1997)

Effects of final state interaction on asymmetries in inclusive scattering of polarized electrons on polarized  $^3\text{He}$  are investigated using a consistent  $^3\text{He}$  bound state wave function and  $3N$  continuum scattering states. Significant effects are found, which influence the extraction of the magnetic neutron form factor from  $A_{T'}$ . The enhancement found experimentally for  $A_{T'}$  near the  $3N$  breakup threshold, which could not be explained in calculations carried through in plane wave impulse approximation up to now, occurs now also in theory if the full final state interaction is included. [S0556-2813(98)02301-2]

PACS number(s): 13.40.Gp, 13.60.Hb, 21.45.+v, 24.70.+s

## I. INTRODUCTION

The electromagnetic form factors of the nucleons are of fundamental interest in nuclear and particle physics. While the proton form factors have been determined from elastic electron-proton scattering over a wide range of momentum transfers with good accuracy [1], this is not the case for the neutron, since no free neutron targets exist. One is therefore forced to extract information on the neutron from electron scattering on light nuclei. Obviously ambiguities arising from nuclear structure and reaction mechanisms should be minimized. So far mainly the deuteron has been used as a target [2]. The  $^3\text{He}$  nucleus has also attracted much attention as an ideal target [3,4]. If one assumes that the  $^3\text{He}$  wave function is spatially symmetric (antisymmetric in spin-isospin space), then the spins of the two protons are coupled to zero and the spin of  $^3\text{He}$  is carried by the neutron alone. Under this simplifying assumption a polarized  $^3\text{He}$  nucleus can be considered to be a polarized neutron. Now this picture of the  $^3\text{He}$  wave function, the so-called principal  $S$ -state approximation, is valid to about 92% with respect to its norm. (This refers to Bonn  $B$  potential [5], which we use in this article.) Motivated by that attractive feature, recently several experiments have been performed, where longitudinally polarized electrons with helicities  $h(=\pm 1)$  have been inclusively scattered on polarized  $^3\text{He}$  targets [6–10]. The aim was to measure the asymmetries

$$A = \frac{\sigma(h=+1) - \sigma(h=-1)}{\sigma(h=+1) + \sigma(h=-1)}, \quad (1)$$

depending on the spin direction of  $^3\text{He}$ . These asymmetries are expected to be sensitive to the electromagnetic form factors of the neutron. The data have been analyzed so far in plane wave impulse approximation [11,12] and based on a single nucleon current operator. That approximation neglects the interaction between the nucleon which absorbed the photon and the two other nucleons.

It is the aim of this investigation to remove that theoretical uncertainty and to treat the  $^3\text{He}$  bound state wave function and the  $3N$  continuum representing the final  $3N$  scattering state on an equal footing, using exact solutions of three-body Faddeev equations based on realistic  $NN$  forces. Our theoretical formalism is described in Sec. II and our results in comparison to the data in Sec. III. A summary is given in Sec. IV.

## II. THEORY

In recent articles [13–17] we studied elastic and inelastic electron scattering on  $^3\text{He}$  corresponding to unpolarized experiments. So far our dynamical picture is a nonrelativistic framework, a single nucleon current operator, and the exact treatment of realistic  $NN$  forces among the three nucleons. For the relatively low momentum transfers considered up to now that picture was quite successful and the final state interaction (FSI) among the three nucleons played a significant role. Now we apply that dynamical picture to the scattering of polarized electrons on polarized  $^3\text{He}$  targets under inclusive conditions. The derivation of the corresponding cross section is known [18]. However to stay in line with the no-

\*Present address: Institut für Kernphysik, Fachbereich 5 der Technischen Hochschule Darmstadt, D-64289 Darmstadt, Germany.

†Present address: Los Alamos National Laboratory, Theoretical Division, Los Alamos, NM 87545.

tation in our previous articles and to show its extensions we just mention the new ingredients. In the evaluation of the cross section the fixed electron polarization in the initial state leads to an additional term proportional to the helicity  $h$  on top of the usual expression for the electron tensor

$$\begin{aligned} L^{\mu\nu} &\equiv \sum_{s'} \bar{u}(k's') \gamma^\mu u(ks) [\bar{u}(k's') \gamma^\nu u(ks)]^* \\ &= \frac{1}{2m^2} (k^\mu k'^\nu + k'^\mu k^\nu - g^{\mu\nu} k \cdot k' + ih \epsilon^{\mu\nu\alpha\beta} k_\alpha k'_\beta). \end{aligned} \quad (2)$$

That additional last term in Eq. (2) has been evaluated under the condition that the electron mass  $m$  can be neglected in relation to its energy. Straightforward contraction with the hadronic tensor yields the inclusive cross section in the lab system

$$\frac{d\sigma}{d\hat{k}' dk_0} = \sigma_{\text{Mott}} [v_L R_L + v_T R_T + h(v_{T'} R_{T'} + v_{TL'} R_{TL'})]. \quad (3)$$

The unprimed terms are the familiar ones for the unpolarized setup [17]. The primed terms are kinematical factors from the electron tensor

$$v_{T'} = \sqrt{\frac{-Q^2}{\tilde{Q}^2} + \tan^2 \frac{\Theta}{2}} \tan \frac{\Theta}{2}, \quad (4)$$

$$v_{TL'} = \frac{1}{\sqrt{2}} \frac{Q^2}{\tilde{Q}^2} \tan \frac{\Theta}{2}, \quad (5)$$

and structure functions related to the hadronic tensor

$$R_{T'} = \sum_{m'\tau'} \int df' \delta(M + \omega - P'_0) (|N_1|^2 - |N_{-1}|^2), \quad (6)$$

$$R_{TL'} = - \sum_{m'\tau'} \int df' \delta(M + \omega - P'_0) 2 \text{Re}[N_0(N_1 + N_{-1})^*]. \quad (7)$$

Here  $Q = (\omega, \vec{Q})$  is the four momentum of the photon,  $\Theta$  the electron scattering angle,  $M$  the target mass, and  $P'_0$  the total energy of the final state. The summation over all spin and isospin magnetic quantum numbers and momenta in the final state is indicated by  $m'$ ,  $\tau'$ , and  $df'$ . The nuclear matrix elements  $N_0$  and  $N_{\pm 1}$  are

$$N_0 = \langle \Psi_{f'm'\tau'}^{(-)} | \rho(\vec{Q}) | \Psi_{3\text{He}} \rangle, \quad (8)$$

$$N_{\pm 1} = \langle \Psi_{f'm'\tau'}^{(-)} | j_{\pm 1}(\vec{Q}) | \Psi_{3\text{He}} \rangle, \quad (9)$$

where  $|\Psi_{3\text{He}}\rangle$  is the  $^3\text{He}$  ground state,  $|\Psi_{f'm'\tau'}^{(-)}\rangle$  a  $3N$  scattering state with the asymptotic quantum numbers  $f'm'\tau'$ ,  $\rho(\vec{Q})$  the electromagnetic hadronic density operator, and  $j_{\pm 1}(\vec{Q})$  the spherical components of the electromagnetic

hadronic current operator. Since we use a nonrelativistic framework, the argument of the  $\delta$  function in Eqs. (6)–(7) is

$$M + \omega - P'_0 = \epsilon_{3\text{He}} + \omega - \frac{\tilde{Q}^2}{6m_N} - E_{f'} \equiv E - E_{f'}, \quad (10)$$

where  $\epsilon_{3\text{He}}$  is the  $^3\text{He}$  binding energy (negative),  $m_N$  the nucleon mass, the final total momentum  $\vec{P}' = \vec{Q}$ , and  $E_{f'}$  the internal  $3N$  energy related to the quantum numbers  $f'$ .

In evaluating the primed structure functions we can generalize a method proposed in [15]. Let us define

$$\begin{aligned} \mathcal{R}_{AB} &\equiv \sum_{m'\tau'} \int df' \delta(E - E_{f'}) \langle \Psi_{f'm'\tau'}^{(-)} | A | \Psi_{3\text{He}} \rangle \\ &\quad \times \langle \Psi_{f'm'\tau'}^{(-)} | B | \Psi_{3\text{He}} \rangle^* \\ &= \sum_{m'\tau'} \int df' \langle \Psi_{3\text{He}} | B^\dagger | \Psi_{f'm'\tau'}^{(-)} \rangle \delta(E - E_{f'}) \\ &\quad \times \langle \Psi_{f'm'\tau'}^{(-)} | A | \Psi_{3\text{He}} \rangle \\ &= \sum_{m'\tau'} \int df' \langle \Psi_{3\text{He}} | B^\dagger \delta(E - H) | \Psi_{f'm'\tau'}^{(-)} \rangle \\ &\quad \times \langle \Psi_{f'm'\tau'}^{(-)} | A | \Psi_{3\text{He}} \rangle \\ &= \langle \Psi_{3\text{He}} | B^\dagger \delta(E - H) A | \Psi_{3\text{He}} \rangle. \end{aligned} \quad (11)$$

We introduced the  $3N$  Hamiltonian  $H$  and used the completeness relation (the ground state does not contribute, since  $E$  lies in the  $3N$  continuum). In our case the operators  $A$  and  $B$  are either  $\rho(\vec{Q})$  or  $j_{\pm 1}(\vec{Q})$ .

In terms of  $\mathcal{R}_{AB}$  the four structure functions can be expressed as

$$R_L = \mathcal{R}_{\rho\rho}, \quad (12)$$

$$R_T = \mathcal{R}_{j_{+1}j_{+1}} + \mathcal{R}_{j_{-1}j_{-1}}, \quad (13)$$

$$R_{T'} = \mathcal{R}_{j_{+1}j_{+1}} - \mathcal{R}_{j_{-1}j_{-1}}, \quad (14)$$

$$R_{TL'} = -2 \text{Re}[\mathcal{R}_{j_{+1}\rho} + \mathcal{R}_{j_{-1}\rho}]. \quad (15)$$

The  $^3\text{He}$  state polarized in the direction  $\theta^*$ ,  $\phi^*$  is

$$|\Psi_{3\text{He}m}\rangle_{\theta^*\phi^*} = \sum_{m'} |\Psi_{3\text{He}m'}\rangle D_{m',m}^{(1/2)}(\phi^*, \theta^*, 0), \quad (16)$$

where  $|\Psi_{3\text{He}m'}\rangle$  is quantized with respect to the  $z$  direction and  $D_{m',m}^{(1/2)}$  is the Wigner  $D$  function [19]. This modifies the expression for  $\mathcal{R}_{AB}$  as

$$\mathcal{R}_{AB} = \sum_{m'} \sum_{m''} D_{m',m}^{(1/2)*} D_{m'',m}^{(1/2)} \mathcal{R}_{AB;m'',m'}, \quad (17)$$

where

$$\mathcal{R}_{AB;m'',m'} = \langle \Psi_{3\text{He}m'} | B^\dagger \delta(E - H) A | \Psi_{3\text{He}m''} \rangle. \quad (18)$$

Using

$$\begin{aligned}
& D_{m',m}^{(1/2)*}(\phi^*, \theta^*, 0) D_{m'',m}^{(1/2)}(\phi^*, \theta^*, 0) \\
&= \sum_J (-)^{m'-m} C\left(\frac{1}{2} \frac{1}{2} J, -m' m''\right) C\left(\frac{1}{2} \frac{1}{2} J, -m, m\right) \\
&\quad \times D_{-m'+m'',0}^{(J)}(\phi^*, \theta^*, 0) \quad (19)
\end{aligned}$$

and the explicit expressions for the  $D$  function

$$D_{m',0}^J(\phi^*, \theta^*, 0) = \sqrt{\frac{4\pi}{2J+1}} Y_{JM}^*(\theta^*, \phi^*), \quad (20)$$

we obtain the following expression for  $\mathcal{R}_{AB}$ :

$$\begin{aligned}
\mathcal{R}_{AB} &= \frac{1}{2} \sum_{m'} \mathcal{R}_{AB;m',m'} \\
&+ \frac{1}{2} \cos \theta^* (\mathcal{R}_{AB; 1/2 \ 1/2} - \mathcal{R}_{AB; -1/2 \ -1/2}) \\
&+ \frac{1}{2} \sin \theta^* (e^{-i\phi^*} \mathcal{R}_{AB; 1/2 \ -1/2} + e^{i\phi^*} \mathcal{R}_{AB; -1/2 \ 1/2}), \quad (21)
\end{aligned}$$

where we have chosen  $m = \frac{1}{2}$ . In other words the  ${}^3\text{He}$  spin points into the direction  $\theta^* \phi^*$ .

If the operators  $A$  and  $B$  are different the method proposed in [15] to evaluate  $\mathcal{R}_{AB;m''m'}$  has to be generalized to

$$\begin{aligned}
\mathcal{R}_{AB;m''m'} &= \frac{1}{2\pi i} \left\langle \Psi_{3\text{He}m'} \left| B^\dagger \frac{1}{E - i\epsilon - H} A \right| \Psi_{3\text{He}m''} \right\rangle \\
&\quad - \frac{1}{2\pi i} \left\langle \Psi_{3\text{He}m'} \left| B^\dagger \frac{1}{E + i\epsilon - H} A \right| \Psi_{3\text{He}m''} \right\rangle \\
&\equiv \frac{1}{2\pi i} \langle \Psi_{3\text{He}m'} | B^\dagger | \Psi_A^{(-)} m'' \rangle \\
&\quad - \frac{1}{2\pi i} \langle \Psi_{3\text{He}m'} | B^\dagger | \Psi_A^{(+)} m'' \rangle. \quad (22)
\end{aligned}$$

We introduced

$$|\Psi_A^{(\pm)} m''\rangle \equiv \frac{1}{E \pm i\epsilon - H} A |\Psi_{3\text{He}m''}\rangle \quad (23)$$

Now

$$\begin{aligned}
& \langle \Psi_{3\text{He}m'} | B^\dagger | \Psi_A^{(-)} m'' \rangle \\
&= \langle \Psi_A^{(-)} m'' | B | \Psi_{3\text{He}m'} \rangle^* \\
&= \left\langle \Psi_{3\text{He}m''} \left| A^\dagger \frac{1}{E + i\epsilon - H} B \right| \Psi_{3\text{He}m'} \right\rangle^* \\
&\equiv \langle \Psi_{3\text{He}m''} | A^\dagger | \Psi_B^{(+)} m' \rangle^* \quad (24)
\end{aligned}$$

with

$$|\Psi_B^{(+)} m'\rangle = \frac{1}{E + i\epsilon - H} B |\Psi_{3\text{He}m'}\rangle. \quad (25)$$

Therefore we get

$$\begin{aligned}
\mathcal{R}_{AB;m''m'} &= \frac{1}{2\pi i} (\langle \Psi_{3\text{He}m''} | A^\dagger | \Psi_B^{(+)} m' \rangle^* \\
&\quad - \langle \Psi_{3\text{He}m'} | B^\dagger | \Psi_A^{(+)} m'' \rangle). \quad (26)
\end{aligned}$$

The states  $|\Psi_{A,B}^{(\pm)} m\rangle$ , defined in Eqs. (23) and (25) contain all the complexity of the interaction among the three nucleons and are evaluated as in [15,17] using the Faddeev scheme. We get

$$|\Psi_C^{(\pm)} m\rangle = G_0(1+P)|U_C m\rangle \quad (27)$$

with

$$|U_C m\rangle = (1+tG_0)C^{(1)}|\Psi_{3\text{He}m}\rangle + tG_0P|U_C m\rangle. \quad (28)$$

Here  $C$  is either  $A$  or  $B$  (for instance  $\rho$  or  $j_{\pm 1}$ ) and we assumed that  $A$  or  $B$  can be decomposed as

$$C = \sum_{i=1}^3 C^{(i)}. \quad (29)$$

Further  $t$  is the  $NN$   $t$  matrix,  $G_0$  the free  $3N$  propagator, and  $P$  the sum of a cyclic and anticyclic permutation of three objects. The Faddeev equation (28) has been introduced and handled numerically before in [17].

Inserting Eq. (28) into Eq. (26) we get

$$\begin{aligned}
\mathcal{R}_{AB;m''m'} &= \frac{1}{2\pi i} (\langle \Psi_{3\text{He}m''} | A^\dagger G_0(1+P) | U_B m' \rangle^* \\
&\quad - \langle \Psi_{3\text{He}m'} | B^\dagger G_0(1+P) | U_A m'' \rangle) \\
&= \frac{3}{2\pi i} (\langle \Psi_{3\text{He}m''} | A^{(1)\dagger} G_0(1+P) | U_B m' \rangle^* \\
&\quad - \langle \Psi_{3\text{He}m'} | B^{(1)\dagger} G_0(1+P) | U_A m'' \rangle). \quad (30)
\end{aligned}$$

In the last step we used Eq. (29) and the fact that the states to the left and right of  $A^\dagger$  or  $B^\dagger$  are antisymmetrical.

Further consideration requires a partial wave decomposition. We introduce our standard basis in momentum space [20]

$$|pq\alpha\mathcal{JM}\rangle = \left| pq(ls)j \left( \lambda \frac{1}{2} \right) J\mathcal{M} \left( t \frac{1}{2} \right) TM_T \right\rangle, \quad (31)$$

where  $p$  and  $q$  are magnitudes of Jacobi momenta and the set of discrete quantum numbers  $\alpha$  comprises angular momenta, spins, and isospins for a three-nucleon system. We indicate the dependence on  $\mathcal{JM}$  explicitly.

Let us introduce

$$\begin{aligned}
\mathcal{S}_{AB;m''m'} &\equiv \langle \Psi_{3\text{He}m'} | B^{(1)\dagger} G_0(1+P) | U_A m'' \rangle \\
&= \oint \frac{1}{E + i\epsilon - p^2/m - (3/4m)q^2} \\
&\quad \times \langle pq\alpha\mathcal{JM} | (1+P) B^{(1)} | \Psi_{3\text{He}m'} \rangle^* \langle pq\alpha\mathcal{JM} | U_A m'' \rangle, \quad (32)
\end{aligned}$$

where the sums in  $\mathfrak{J}$  include the summation over the magnetic quantum number  $M$  of the total  $3N$  angular momentum  $\mathcal{J}$ . Equation (30) is then expressed as

$$\mathcal{R}_{AB;m''m'} = \frac{3}{2\pi i} (\mathcal{S}_{BA;m''m'}^* - \mathcal{S}_{AB;m''m'}). \quad (33)$$

Since we choose the  $z$  axis to lie in the direction  $\hat{Q}$  of the virtual photon, the density operator  $\rho^{(1)}$  conserves the  $3N$  magnetic quantum number [17], while  $j_{+1}$  ( $j_{-1}$ ) increases (decreases) the magnetic quantum number by 1. This leads to the following conditions:

$$\begin{aligned} \langle pq\alpha\mathcal{JM} | (1+P)\rho^{(1)} | \Psi_{3\text{He}}m \rangle \\ = \delta_{M,m} \langle pq\alpha\mathcal{JM} | (1+P)\rho^{(1)} | \Psi_{3\text{He}}m \rangle, \end{aligned} \quad (34)$$

$$\langle pq\alpha\mathcal{JM} | U_\rho m \rangle = \delta_{M,m} \langle pq\alpha\mathcal{JM} | U_\rho m \rangle, \quad (35)$$

$$\begin{aligned} \langle pq\alpha\mathcal{JM} | (1+P)j_{\pm 1}^{(1)} | \Psi_{3\text{He}}m \rangle \\ = \delta_{M,m\pm 1} \langle pq\alpha\mathcal{JM} | (1+P)j_{\pm 1}^{(1)} | \Psi_{3\text{He}}m \rangle, \end{aligned} \quad (36)$$

$$\langle pq\alpha\mathcal{JM} | U_{j_{\pm 1}} m \rangle = \delta_{M,m\pm 1} \langle pq\alpha\mathcal{JM} | U_{j_{\pm 1}} m \rangle. \quad (37)$$

As a consequence the only nonzero expressions  $\mathcal{S}_{AB;m''m'}$  are

$$\begin{aligned} \mathcal{S}_{\rho\rho;1/2\ 1/2}, \quad \mathcal{S}_{\rho\rho;-1/2\ -1/2}, \\ \mathcal{S}_{j_{\pm 1}j_{\pm 1};1/2\ 1/2}, \quad \mathcal{S}_{j_{\pm 1}j_{\pm 1};-1/2\ -1/2}, \\ \mathcal{S}_{j_{+1}\rho;-1/2\ 1/2}, \quad \mathcal{S}_{j_{-1}\rho;1/2\ -1/2}, \\ \mathcal{S}_{\rho j_{+1};1/2\ -1/2}, \quad \mathcal{S}_{\rho j_{-1};-1/2\ 1/2}. \end{aligned} \quad (38)$$

Now a detailed look into the partial wave decomposed forms [17] reveals the following symmetry properties:

$$\begin{aligned} \left\langle pq\alpha\mathcal{J} - \frac{1}{2} \left| (1+P)\rho^{(1)} \right| \Psi_{3\text{He}} - \frac{1}{2} \right\rangle \\ = (-1)^{\mathcal{J} - 1/2} \Pi \left\langle pq\alpha\mathcal{J} \frac{1}{2} \left| (1+P)\rho^{(1)} \right| \Psi_{3\text{He}} \frac{1}{2} \right\rangle, \end{aligned} \quad (39)$$

$$\left\langle pq\alpha\mathcal{J} - \frac{1}{2} \left| U_\rho - \frac{1}{2} \right\rangle = (-1)^{\mathcal{J} - 1/2} \Pi \left\langle pq\alpha\mathcal{J} \frac{1}{2} \left| U_\rho \frac{1}{2} \right\rangle, \quad (40)$$

$$\begin{aligned} \left\langle pq\alpha\mathcal{J} - \frac{1}{2} \left| (1+P)j_{-1}^{(1)} \right| \Psi_{3\text{He}} \frac{1}{2} \right\rangle \\ = (-1)^{\mathcal{J} - 1/2} \Pi \left\langle pq\alpha\mathcal{J} \frac{1}{2} \left| (1+P)j_{+1}^{(1)} \right| \Psi_{3\text{He}} - \frac{1}{2} \right\rangle, \end{aligned} \quad (41)$$

$$\begin{aligned} \left\langle pq\alpha\mathcal{J} - \frac{1}{2} \left| UU_{j_{-1}} \frac{1}{2} \right\rangle \\ = (-1)^{\mathcal{J} - 1/2} \Pi \left\langle pq\alpha\mathcal{J} \frac{1}{2} \left| U_{j_{+1}} - \frac{1}{2} \right\rangle, \end{aligned} \quad (42)$$

$$\begin{aligned} \left\langle pq\alpha\mathcal{J} - \frac{3}{2} \left| (1+P)j_{-1}^{(1)} \right| \Psi_{3\text{He}} - \frac{1}{2} \right\rangle \\ = (-1)^{\mathcal{J} - 1/2} \Pi \left\langle pq\alpha\mathcal{J} \frac{3}{2} \left| (1+P)j_{+1}^{(1)} \right| \Psi_{3\text{He}} \frac{1}{2} \right\rangle, \end{aligned} \quad (43)$$

$$\left\langle pq\alpha\mathcal{J} - \frac{3}{2} \left| U_{j_{-1}} - \frac{1}{2} \right\rangle = (-1)^{\mathcal{J} - 1/2} \Pi \left\langle pq\alpha\mathcal{J} \frac{3}{2} \left| U_{j_{+1}} \frac{1}{2} \right\rangle, \quad (44)$$

where  $\Pi$  is the parity of the state  $|pq\alpha\rangle$ .

As a consequence of Eqs. (39)–(44),

$$\mathcal{S}_{\rho\rho;-1/2\ -1/2} = \mathcal{S}_{\rho\rho;1/2\ 1/2}, \quad (45)$$

$$\mathcal{S}_{j_{-1}j_{-1};\pm 1/2\ \pm 1/2} = \mathcal{S}_{j_{+1}j_{+1};\mp 1/2\ \mp 1/2}, \quad (46)$$

$$\mathcal{S}_{j_{-1}\rho;1/2\ -1/2} = \mathcal{S}_{j_{+1}\rho;-1/2\ 1/2}, \quad (47)$$

$$\mathcal{S}_{\rho j_{-1};-1/2\ 1/2} = \mathcal{S}_{\rho j_{+1};1/2\ -1/2}. \quad (48)$$

Further, using Eq. (33) one gets

$$\mathcal{R}_{\rho\rho;1/2\ 1/2} = \mathcal{R}_{\rho\rho;-1/2\ -1/2} = -\frac{3}{\pi} \text{Im } \mathcal{S}_{\rho\rho;1/2\ 1/2}, \quad (49)$$

$$\begin{aligned} \mathcal{R}_{j_{+1}j_{+1};\pm 1/2\ \pm 1/2} = \mathcal{R}_{j_{-1}j_{-1};\mp 1/2\ \mp 1/2} \\ = -\frac{3}{\pi} \text{Im } \mathcal{S}_{j_{+1}j_{+1};\pm 1/2\ \pm 1/2}, \end{aligned} \quad (50)$$

$$\begin{aligned} \mathcal{R}_{j_{+1}\rho;-1/2\ 1/2} = \mathcal{R}_{j_{-1}\rho;1/2\ -1/2} \\ = \frac{3}{2\pi i} (\mathcal{S}_{\rho j_{+1};1/2\ -1/2} - \mathcal{S}_{j_{+1}\rho;-1/2\ 1/2}). \end{aligned} \quad (51)$$

The final step is to use Eqs. (12)–(15) and (21) to arrive at

$$R_L = \mathcal{R}_{\rho\rho;1/2\ 1/2}, \quad (52)$$

$$R_T = \mathcal{R}_{j_{+1}j_{+1};1/2\ 1/2} + \mathcal{R}_{j_{+1}j_{+1};-1/2\ -1/2}, \quad (53)$$

$$R_{T'} = \cos \theta^* (\mathcal{R}_{j_{+1}j_{+1};1/2\ 1/2} - \mathcal{R}_{j_{+1}j_{+1};-1/2\ -1/2}), \quad (54)$$

$$R_{TL'} = -\sin \theta^* \cos \phi^* 2 \text{Re}(\mathcal{R}_{j_{+1}\rho;-1/2\ 1/2}). \quad (55)$$

For easier use we display in the Appendix the explicit expressions for the four structure functions (52)–(55) using Eqs. (32) and (49)–(51). The partial wave projected matrix elements occurring therein are evaluated according to our standard techniques [13–17].

The only structure functions depending on  $\theta^*$  and  $\phi^*$  are

$$R_{T'} \equiv \bar{R}_{T'} \cos \theta^*, \quad (56)$$

$$R_{TL'} \equiv \bar{R}_{TL'} \sin \theta^* \cos \phi^*. \quad (57)$$

Then according to Eqs. (1) and (3) the asymmetries are

$$A \equiv \frac{d\sigma/d\hat{k}'dk'_0|_{h=1} - d\sigma/d\hat{k}'dk'_0|_{h=-1}}{d\sigma/d\hat{k}'dk'_0|_{h=1} + d\sigma/d\hat{k}'dk'_0|_{h=-1}} \\ = \frac{v_{T'}\tilde{R}_{T'} \cos \theta^* + v_{TL'}\tilde{R}_{TL'} \sin \theta^* \cos \phi^*}{v_L R_L + v_T R_T}. \quad (58)$$

Putting the angle  $\theta^*$  between the direction of the  ${}^3\text{He}$  target spin ( $m = \frac{1}{2}$ ) and the direction  $\hat{Q}$  of the virtual photon to zero one selects the transverse asymmetry  $A_{T'}$  (proportional to  $\tilde{R}_{T'}$ ), whereas putting that angle to  $90^\circ$  one gets the transverse-longitudinal asymmetry  $A_{TL'}$  (proportional to  $\tilde{R}_{TL'}$ ).

Let us now regard the most simplified picture. We neglect all final state interactions, thereby excluding also the  $pd$  breakup channel. Also the antisymmetrization is kept only in the two-body subsystem described by  $\vec{p}$ . Finally we restrict the  ${}^3\text{He}$  wave function to the principal  $S$  state. In order to define clearly our notation we start from the matrix elements for the symmetrized plane wave impulse approximation (PWIAS)

$$N_{\text{PWIAS}}^\mu \equiv \frac{1}{\sqrt{3!}} \langle \vec{p}\vec{q}m_1m_2m_3\tau_1\tau_2\tau_3 | (1 - P_{23})(1 + P)j^\mu(\vec{Q}) \\ \times |\Psi_{{}^3\text{He}}m\rangle_{\theta^*\phi^*} \\ = \frac{3}{\sqrt{3!}} \langle \vec{p}\vec{q}m_1m_2m_3\tau_1\tau_2\tau_3 | (1 - P_{23})(1 + P)j_{(1)}^\mu(\vec{Q}) \\ \times |\Psi_{{}^3\text{He}}m\rangle_{\theta^*\phi^*}. \quad (59)$$

As before we reduced the single nucleon current operator to one term. The subscript 1 indicates the particle number, which in our notation is described by  $\vec{q}$ . Now we drop the permutation operator  $P$ , apply  $P_{23}$ , and insert the principal  $S$ -state approximation. The resulting nuclear matrix elements are

$$\tilde{N}_0 \equiv \sqrt{6} \langle \vec{p}\vec{q}m_1m_2m_3\tau_1\tau_2\tau_3 | \rho^{(1)}(\vec{Q}) |\Psi_{{}^3\text{He}}^{PS}m\rangle_{\theta^*\phi^*}, \quad (60)$$

$$\tilde{N}_\pm \equiv \sqrt{6} \langle \vec{p}\vec{q}m_1m_2m_3\tau_1\tau_2\tau_3 | j_\pm^{(1)}(\vec{Q}) |\Psi_{{}^3\text{He}}^{PS}m\rangle_{\theta^*\phi^*}. \quad (61)$$

The principal  $S$  state is

$$|\Psi_{{}^3\text{He}}^{PS}m\rangle = |\phi_S\rangle |\xi_a m\rangle, \quad (62)$$

where  $|\xi_a m\rangle$  is the totally antisymmetrical spin-isospin state

$$|\xi_a m\rangle = \frac{1}{\sqrt{2}} \left[ \left( \left| t=0 \frac{1}{2} \right\rangle T = \frac{1}{2} \right) \left( \left| s=1 \frac{1}{2} \right\rangle S = \frac{1}{2} m \right) \right. \\ \left. - \left( \left| t=1 \frac{1}{2} \right\rangle T = \frac{1}{2} \right) \left( \left| s=0 \frac{1}{2} \right\rangle S = \frac{1}{2} m \right) \right] \quad (63)$$

and  $|\phi_S\rangle$  is the totally symmetrical space part belonging to total orbital angular momentum  $L=0$ . In terms of our standard notation [20] one easily gets

$$|\Psi_{{}^3\text{He}}^{PS}m\rangle = \sum_{l \text{ even}} \sum_{s,t} \int dp p^2 \int dq q^2 \\ \times \left| pq(l)0 \left( s \frac{1}{2} \right) S = \frac{1}{2} m \left( t \frac{1}{2} \right) T = \frac{1}{2} \right\rangle \\ \times \phi_l(pq) \frac{1}{\sqrt{2}} (\delta_{s1}\delta_{t0} - \delta_{s0}\delta_{t1}) \quad (64)$$

with

$$\phi_l(pq) = \frac{1}{\sqrt{2}} (\Psi_{(l)0(1/2)1/2(0/2)1/2}(pq) \\ - \Psi_{(l)0(0/2)1/2(1/2)1/2}(pq)) \quad (65)$$

and  $\Psi_\alpha(pq)$  are the wave function components  $\langle pq\alpha | \Psi m \rangle$  determined in the Faddeev scheme. Using Eqs. (16) and (62) the nuclear matrix elements (60) and (61) turn into

$$\tilde{N}_0 = \sqrt{6} F_1^{(\tau_1)}(\vec{Q}) \sum_{m'} D_{m',m}^{(1/2)} \phi_S \left( \vec{p}, \vec{q} - \frac{2}{3} \vec{Q} \right) \\ \times \langle m_1 m_2 m_3 \tau_1 \tau_2 \tau_3 | \xi_a m' \rangle, \quad (66)$$

$$\tilde{N}_{\pm 1} = \sqrt{6} F_1^{(\tau_1)}(\vec{Q}) \frac{q_{\pm 1}}{m_N} \sum_{m'} D_{m',m}^{(1/2)} \phi_S \left( \vec{p}, \vec{q} - \frac{2}{3} \vec{Q} \right) \\ \times \langle m_1 m_2 m_3 \tau_1 \tau_2 \tau_3 | \xi_a m' \rangle - \sqrt{12} G_M^{(\tau_1)} \\ \times (\vec{Q}) \frac{|\vec{Q}|}{2m_N} \sum_{m'} D_{m',m}^{(1/2)} \phi_S \left( \vec{p}, \vec{q} - \frac{2}{3} \vec{Q} \right) \\ \times \langle m_1 \mp 1 m_2 m_3 \tau_1 \tau_2 \tau_3 | \xi_a m' \rangle. \quad (67)$$

Thereby the single particle current operator has been chosen according to [14]. Despite the approximate, not fully antisymmetrized final state in Eqs. (60) and (61), we stick to the summation prescription over all final states in the evaluation of the structure functions, which corresponds to the fully antisymmetrized final states in Eq. (59):

$$\mathcal{F} \equiv \frac{1}{6} \sum_{m_1 m_2 m_3} \sum_{\tau_1 \tau_2 \tau_3} \int d\vec{p} d\vec{q}. \quad (68)$$

Then a straightforward evaluation yields

$$R_L = \frac{2m_N}{3} \int_0^{p_{\max}} dp p^2 q \int d\hat{p} \int d\hat{q} \left| \phi_S \left( \vec{p}, \vec{q} - \frac{2}{3} \vec{Q} \right) \right|^2 \\ \times \left( \frac{1}{3} [F_1^{(n)}(\vec{Q})]^2 + \frac{2}{3} [F_1^{(p)}(\vec{Q})]^2 \right), \quad (69)$$

$$R_T = \frac{2m_N}{3} \int_0^{p_{\max}} dp p^2 q \int d\hat{p} \int d\hat{q} \left| \phi_S \left( \vec{p}, \vec{q} - \frac{2}{3} \vec{Q} \right) \right|^2 \times \left[ \frac{8\pi}{9} \frac{|\vec{q}|^2}{m_N^2} |Y_{1,1}(\hat{q})|^2 \{ [F_1^{(n)}(\vec{Q})]^2 + 2[F_1^{(p)}(\vec{Q})]^2 \} + \left( \frac{2}{3} [G_M^{(n)}(\vec{Q})]^2 + \frac{4}{3} [G_M^{(p)}(\vec{Q})]^2 \right) \frac{|\vec{Q}|^2}{4m_N^2} \right], \quad (70)$$

$$R_{T'} = \frac{2m_N}{3} \int_0^{p_{\max}} dp p^2 q \int d\hat{p} \int d\hat{q} \left| \phi_S \left( \vec{p}, \vec{q} - \frac{2}{3} \vec{Q} \right) \right|^2 \times \left( -\frac{1}{6} \cos \theta^* \right) [G_M^{(n)}(\vec{Q})]^2 \frac{|\vec{Q}|^2}{m_N^2}, \quad (71)$$

$$R_{TL'} = \frac{2m_N}{3} \int_0^{p_{\max}} dp p^2 q \int d\hat{p} \int d\hat{q} \left| \phi_S \left( \vec{p}, \vec{q} - \frac{2}{3} \vec{Q} \right) \right|^2 \times \frac{\sqrt{2}}{3} F_1^{(n)}(\vec{Q}) G_M^{(n)}(\vec{Q}) \frac{|\vec{Q}|}{m_N} \cos \phi^* \sin \theta^*. \quad (72)$$

The energy conserving delta function gives  $p_{\max}$  and  $q$  to be

$$p_{\max} = \sqrt{m_N E}, \quad (73)$$

$$q = \sqrt{\frac{4}{3}(p_{\max}^2 - p^2)}. \quad (74)$$

Note that  $R_L$  and  $R_T$  receive contributions from neutrons and protons, whereas due to the principal  $S$ -state assumption  $R_{T'}$  and  $R_{TL'}$  are fed only by the neutron contribution. It results in the asymmetry

$$A = \left[ v_{T'} \left( -\frac{1}{6} \cos \theta^* \right) [G_M^{(n)}(\vec{Q})]^2 \frac{|\vec{Q}|^2}{m_N^2} + v_{TL'} \frac{\sqrt{2}}{3} F_1^{(n)}(\vec{Q}) G_M^{(n)}(\vec{Q}) \frac{|\vec{Q}|}{m_N} \cos \phi^* \sin \theta^* \right] / \left[ v_L \left( \frac{1}{3} [F_1^{(n)}(\vec{Q})]^2 + \frac{2}{3} [F_1^{(p)}(\vec{Q})]^2 \right) + v_T \left\{ [F_1^{(n)}(\vec{Q})]^2 + 2[F_1^{(p)}(\vec{Q})]^2 \right\} \alpha(\omega, |\vec{Q}|) + \left( \frac{2}{3} [G_M^{(n)}(\vec{Q})]^2 + \frac{4}{3} [G_M^{(p)}(\vec{Q})]^2 \right) \frac{|\vec{Q}|^2}{4m_N^2} \right], \quad (75)$$

where

$$\alpha(\omega, |\vec{Q}|) = \frac{(8\pi/9) \int_0^{p_{\max}} dp p^2 q \int d\hat{p} \int d\hat{q} \left| \phi_S \left[ \vec{p}, \vec{q} - (2/3) \vec{Q} \right] \right|^2 |\vec{q}|^2 / m_N^2 |Y_{1,1}(\hat{q})|^2}{\int_0^{p_{\max}} dp p^2 q \int d\hat{p} \int d\hat{q} \left| \phi_S \left[ \vec{p}, \vec{q} - (2/3) \vec{Q} \right] \right|^2} = \frac{1}{3} \frac{\int_0^{p_{\max}} dp p^2 q (q^2 / m_N^2) \Sigma_i \int_{-1}^1 dx (1-x^2) \phi_i^2 [p, |\vec{q} - (2/3) \vec{Q}|]}{\int_0^{p_{\max}} dp p^2 q \Sigma_i \int_{-1}^1 dx \phi_i^2 [p, |\vec{q} - (2/3) \vec{Q}|]} \quad (76)$$

with  $x = \hat{q} \cdot \hat{Q}$ .

That factor  $\alpha(\omega, |\vec{Q}|)$  is due to the convection current, whose contribution survives solely in  $R_T$  and prevents that the dependence on the  ${}^3\text{He}$  wave function drops out. It is typically of the order  $10^{-3}$ , and together with  $F_1^2(\vec{Q})$  of neutron and proton it is negligible in relation to the other term at the momentum transfer  $|\vec{Q}|$  considered.

If we insert the explicit expressions for the kinematical factors  $v$  and use the nonrelativistic approximation  $Q^2 \approx -\vec{Q}^2$  we get

$$A = \frac{(Q^2/2m_N^2) \tan(\Theta/2) [\sqrt{(-Q^2/\vec{Q}^2) + \tan^2(\Theta/2)} (G_M^{(n)})^2 \cos \theta^* + (2m_N/|\vec{Q}|) F_1^{(n)} G_M^{(n)} \cos \phi^* \sin \theta^*]}{(F_1^{(n)})^2 + 2(F_1^{(p)})^2 - (Q^2/4m_N^2) \{ (G_M^{(n)})^2 + 2(G_M^{(p)})^2 + \alpha(6m_N^2/|\vec{Q}|^2) [(F_1^{(n)})^2 + 2(F_1^{(p)})^2] \}} [1 + 2 \tan^2(\Theta/2)]}, \quad (77)$$

where we kept  $(-Q^2/\vec{Q}^2)$  under the square root in order to facilitate the comparison to the asymmetry gained by scattering a polarized electron on a polarized nucleon target. That well-known expression is

TABLE I. The experimental setup of Refs. [8–10].

|           | $k_0$<br>(MeV) | $\Theta$<br>( $^\circ$ ) | $\theta_A$<br>( $^\circ$ ) | $\phi_A$<br>( $^\circ$ ) | $\omega$<br>(MeV) | $\omega_{\text{QE}}$<br>(MeV) | $Q_{\text{QE}}$<br>(MeV/c) | $\theta_{\text{QE}}^*$<br>( $^\circ$ ) | $\phi_{\text{QE}}^*$<br>( $^\circ$ ) |
|-----------|----------------|--------------------------|----------------------------|--------------------------|-------------------|-------------------------------|----------------------------|----------------------------------------|--------------------------------------|
| Ref. [8]  | 370            | 91.4                     | 42.5                       | 180                      | 91–150            | 107                           | 460                        | 8.9                                    | 180                                  |
| Ref. [9]  | 370            | 70.1                     | 42.5                       | 0                        | 73–97             | 76                            | 386                        | 88.1                                   | 0                                    |
| Ref. [10] | 370            | 70.1                     | 42.5                       | 0                        | 40–52             | 76                            | 386                        | 88.1                                   | 0                                    |

$$A_{\text{nuc}} = \frac{(Q^2/2m_N^2)\tan(\Theta/2)[\sqrt{(-Q^2/\vec{Q}^2) + \tan^2(\Theta/2)G_M^2} \cos \theta^* + (2m_N/|\vec{Q}|)G_E G_M \cos \phi^* \sin \theta^*][1 - (Q^2/4m_N^2)]}{G_E^2 - (Q^2/4m_N^2)G_M^2[1 + 2(1 - Q^2/4m_N^2)]\tan^2(\Theta/2)}. \quad (78)$$

The numerators in Eqs. (77) and (78) are equal except that we use  $F_1$  instead of  $G_E$ . Our single nucleon current operator [14] contains  $F_1$ . In the denominator of Eq. (77), however, there are also contributions from the protons in  $^3\text{He}$  and the correction term  $\alpha$  resulting from the convection current. In  $^3\text{He}$  the nucleons are moving in contrast to the case of a fixed single nucleon target.

Regarding the expression (77) we see that the transverse asymmetry  $A_{T'}$  defined for  $\theta^*=0^\circ$  is proportional to  $(G_M^{(n)})^2$ , whereas the transverse-longitudinal asymmetry  $A_{TL'}$  defined for  $\theta^*=90^\circ$  is proportional to  $F_1^{(n)}G_M^{(n)}$ . Will that simple result survive under more realistic conditions? This is just the aim of our study to learn how a more realistic  $^3\text{He}$  wave function, the inclusion of antisymmetrization in the final state, and the inclusion of final state interactions among the three final nucleons modifies that simple picture and whether these modifications will still leave sufficient sensitivity to the value of the magnetic form factor  $G_M^{(n)}$  of the neutron.

Let us now define the various levels of evaluating the two asymmetries  $A_{T'}$  and  $A_{TL'}$ . The form (77) based on the principal  $S$  state and plane wave impulse approximation without antisymmetrization in the final state [see Eqs. (60)–(61)] will be denoted by PWIA (PS). If we include the realistic  $^3\text{He}$  wave function we denote the result by PWIA. The corresponding structure functions are determined by Eq. (30) dropping the factor 3, the permutation operator  $P$ , and  $U_B$  and  $U_A$  should be chosen by Eq. (28) without the two terms proportional to the  $NN$   $t$  matrix  $t$ . If one restricts  $|\Psi_{^3\text{He}}\rangle$  to the principal  $S$  state the results should be identical to the structure functions evaluated according to Eqs. (69)–(72) and to the asymmetry from Eq. (77). This is a very nontrivial check and turned out to be very well fulfilled.

The next improvement of the theory is to keep plane waves in the final state but antisymmetrize them correctly. This is achieved using Eq. (30) and dropping only in the  $U$  amplitudes of Eq. (28) the terms proportional to  $t$ . This approximation will be denoted by PWIAS.

An intermediate step for including the full final state interaction is to keep in the nuclear matrix elements the interaction in the pair of nucleons which are spectators to the absorption process of the photon on the third nucleon. This approximation is described by the nuclear matrix elements

$$N_{0'} = \sqrt{6}\langle \vec{p}\vec{q}m'_1m'_2m'_3 | (1+tG_0)\rho^{(1)}(\vec{Q}) | \Psi_{^3\text{He}}m \rangle_{\theta^*\phi^*}, \quad (79)$$

$$N_{\pm'} = \sqrt{6}\langle \vec{p}\vec{q}m'_1m'_2m'_3 | (1+tG_0)j_{\pm}^{(1)}(\vec{Q}) | \Psi_{^3\text{He}}m \rangle_{\theta^*\phi^*}, \quad (80)$$

for the  $ppn$ -breakup process and by

$$N_{0,d'} = \langle \varphi_d \vec{q}m'_1m'_d | \rho^{(1)}(\vec{Q}) | \Psi_{^3\text{He}}m \rangle_{\theta^*\phi^*}, \quad (81)$$

$$N_{\pm 1,d'} = \langle \varphi_d \vec{q}m'_1m'_d | j_{\pm}^{(1)}(\vec{Q}) | \Psi_{^3\text{He}}m \rangle_{\theta^*\phi^*}, \quad (82)$$

for the  $pd$ -breakup process. Note that we did not antisymmetrize the final state except in the two-body subsystem. This leads to the expression (30) without the factor 3 and the permutation operator  $P$ , and the  $U$  amplitudes are just given by the driving term in Eq. (28). The corresponding results will be denoted by PWIA'. If on top of that we antisymmetrize the final state the result will be denoted by PWIAS'. This is evaluated using Eq. (30) as it is, but the  $U$  amplitude as for PWIA'. Finally evaluating Eqs. (28) and (30) exactly and thus including the final state interaction to all orders and between all three nucleons, as well as including the antisymmetrization fully will be denoted by full.

### III. RESULTS

We used the Bonn  $B$   $NN$  potential [5] and kept its force components up to total two-nucleon angular momentum  $j=2$  in the treatment of the  $3N$  continuum. The effects of the  $j=3$  components stayed below the percentage level. The electromagnetic nucleon form factors are from [21].

The experimental setup for the spin-dependent asymmetry can be characterized by the initial electron energy ( $k_0$ ), the electron scattering angle ( $\Theta$ ), two angles which parametrize the direction of the target polarization ( $\theta_A, \phi_A$ ) (see Fig. 7 of Ref. [11], e.g.), and the measured energy transfer ( $\omega$ ). These values used in the recent experiments [8–10] are summarized in Table I, together with energy transfer ( $\omega_{\text{QE}}$ ), three-momentum transfer ( $|\vec{Q}|_{\text{QE}}$ ) and the angles defining the polarization with respect to the direction  $\hat{Q}$  of the three-momentum transfer ( $\theta_{\text{QE}}^*$  and  $\phi_{\text{QE}}^*$ ) at the quasielastic (QE) condition. The asymmetry measured in Ref. [8] near the quasielastic kinematics is essentially the transverse asymme-

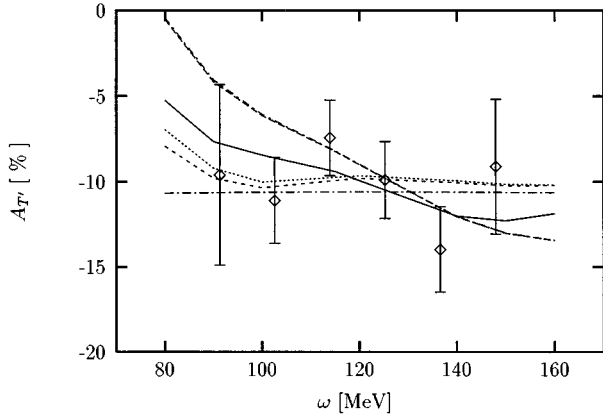


FIG. 1. The transverse asymmetry  $A_{T'}$  as a function of  $\omega$ . The data are from Ref. [8]. The six theoretical curves are PWIA(PS) (dashed-dotted), PWIA (dotted), PWIAS (short dashed), PWIA' (long dashed), PWIAS' (dashed-dotted, declined curve), and full (solid). Note PWIA' and PWIAS' overlap.

try  $A_{T'}$  because of the condition,  $\theta^* \approx 0^\circ$ , and then is expected to be sensitive to the neutron magnetic form factor. Thus hereafter the asymmetry measured in this experiment will be referred to as simply  $A_{T'}$ . On the other hand, those measured near the quasielastic kinematics [9] and a lower- $\omega$  region just above the three-body breakup threshold [10] are essentially the transverse-longitudinal asymmetry  $A_{TL'}$  because of the condition  $\theta^* \approx 90^\circ$ , and then are expected to be sensitive to both of the neutron charge and magnetic form factors. Hereafter the asymmetry measured in these experiments will be referred to as simply  $A_{TL'}$ . These experimental results were analyzed by recent theoretical works [11,12] with realistic  ${}^3\text{He}$  wave functions and plane wave impulse approximation. In this article we call that approximation PWIA'. In Ref. [8], the neutron magnetic form factor  $G_M^n$  was extracted based on PWIA' with reasonable agreement with experimental data. On the other hand, agreement between the PWIA' calculations and the measured asymmetries in Refs. [9,10] is rather poor. The PWIA' prediction of the asymmetry in the quasielastic region was found to be large compared to the experimental data [9] at the  $(1-2.5)\sigma$  level. At the lower  $\omega$  region [10], the experimental asymmetry was found to be enhanced in contradiction with PWIA' calculations.

Let us now regard our results in comparison to the experimental data for  $A_{T'}$  in Fig. 1 and for  $A_{TL'}$  in Fig. 2. We display six theoretical curves. The most naive prediction PWIA(PS) lies within the error bars for four of the six data points for  $A_{T'}$  in Fig. 1. In case of  $A_{TL'}$  shown in Fig. 2 that prediction is essentially zero and clearly disagrees with the data. Replacing the principal  $S$ -state approximation of  ${}^3\text{He}$  by the full expression, called PWIA, causes a visible change for  $A_{T'}$  at low  $\omega$ 's and a much larger one for  $A_{TL'}$ . Now for  $A_{TL'}$  one deviates even stronger from the data. Apparently  $R_{TL'}$  is more sensitive to the  ${}^3\text{He}$  wave function than  $R_{T'}$ . Symmetrizing the final state using PWIAS has a small effect for  $A_{T'}$  but a big one on  $A_{TL'}$ . It rises  $A_{TL'}$  for small  $\omega$ 's qualitatively similar to what happens in the data but misses the data around  $\omega = 60-70$  MeV. A strong move occurs by keeping the final state interaction among the two spectator

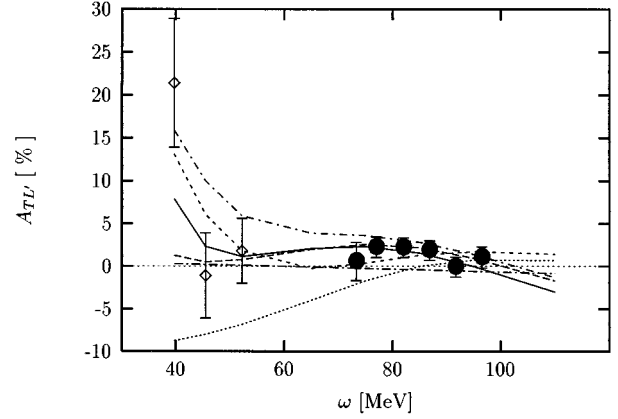


FIG. 2. The transverse-longitudinal asymmetry  $A_{TL'}$  as a function of  $\omega$ . The data ( $\diamond$ ) are from Ref. [9] and the data ( $\bullet$ ) from Ref. [10]. Curves as in Fig 1. The PWIAS' curve rises to the data point at  $\omega = 40$  MeV.

nucleons PWIA'. For lower  $\omega$ 's it appears to be somewhat too high for  $A_{T'}$  and again at low  $\omega$ 's near the threshold for  $3N$  breakup it does not show the quick rise of the one data point in  $A_{TL'}$ . However between 50 and 100 MeV it follows the data for  $A_{TL'}$ . Now symmetrizing in addition the final state PWIAS', it does not cause a visible change for  $A_{T'}$ , but overshoots now the data for  $A_{TL'}$  for  $\omega$ 's below about 70 MeV. Finally the full calculation leads again to a strong shift and agrees now quite well with the data for both  $A_{T'}$  and  $A_{TL'}$ . At very low  $\omega$ 's it now follows the experimental trend for  $A_{TL'}$  though still misses the error bar of the last data point to the left. More precise data for  $A_{TL'}$ , especially in that region would be of interest to quantitatively challenge our present day understanding of final state interactions but possibly also effects related to the choice of the current operator.

Though the data show still some scatter for  $A_{T'}$ , we would like to quantify these results by providing a  $\chi^2$  for  $A_{T'}$ :

$$\chi^2 \equiv \sum_i \frac{[A_{T'}^{\text{theory}}(i) - A_{T'}^{\text{exp}}(i)]^2}{[\Delta A_{T'}^{\text{exp}}(i)]^2}. \quad (83)$$

The sum runs over the six data points. They are 4.2, 4.1, 4.0, 6.1, 6.3, 3.4 for PWIA(PS), PWIA, PWIAS, PWIA', PWIAS', and full, respectively. The full calculation describes the data best and the correct antisymmetrization and the treatment of the full final state interaction is required to achieve quantitative insight. Note that the often used plane wave impulse approximation, here called PWIA' is insufficient.

The aim of the experiments were to achieve information on the magnetic neutron form factor. Therefore the influence of the badly known electric form factor of the neutron  $G_E^{(n)}$  or in our nonrelativistic form  $F_1^{(n)}$  should be known. We restrict our investigation to  $A_{T'}$  and in addition to PWIA(PS) and PWIAS. As an extreme assumption we put  $F_1^{(n)}$  to zero, the effect on  $A_{T'}$  was negligible (below 1%). We expect that this remains true even for the full calculation and therefore we expect that the specific choice of  $F_1^{(n)}$  will not influence significantly the extraction of information on  $G_M^{(n)}$  from  $A_{T'}$ .



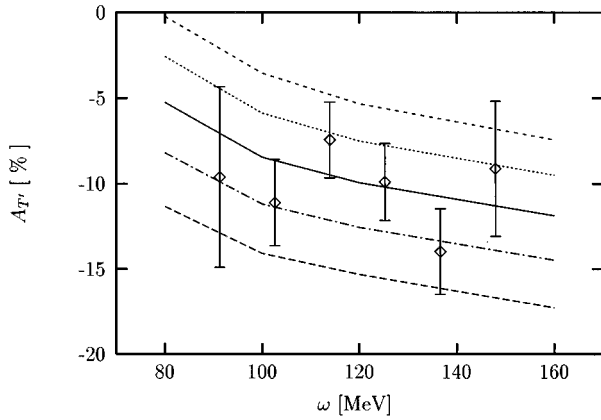


FIG. 3. The dependence of the transverse asymmetry  $A_{T'}$  in the full calculation on the strength factor  $f$  multiplied to the neutron magnetic form factor  $G_M^{(n)}$  from [21].  $f=0.7$  (short-dashed),  $f=0.85$  (dotted),  $f=1$  (solid),  $f=1.15$  (dashed-dotted), and  $f=1.3$  (long-dashed). Comparison to data from [8].

We add the remark that this extreme assumption puts  $A_{TL'}=0$  for PWIA(PS), of course. Obviously the data are different from zero and  $A_{TL'}$  receives contributions from ingredients, which go beyond that most simplistic picture. This can already be seen comparing PWIA(PS) and PWIA in Fig. 2. The difference is just the replacement of the principal  $S$  state  ${}^3\text{He}$  wave function by the realistic one. Apparently the  $S'$ - and  $D$ -state pieces contribute very strongly to  $A_{TL'}$ . This was noticed before in [11].

Being free of that dependence on  $F_1^{(n)}$  for  $A_{T'}$ , we now altered the neutron magnetic form factor by  $\pm 15\%$  and  $\pm 30\%$  and achieved the results, for the full calculation displayed in Fig. 3. Clearly  $\pm 30\%$  changes lie outside the bulk of the data and also  $\pm 15\%$  changes are not acceptable given the data. One can quantify these studies and extract the optimal  $f$  factor multiplying the neutron magnetic form factor  $G_M^{(n)}$  of [21] such that  $\chi^2$  is minimal. This study was performed for the full calculation. We display the resulting  $\chi^2$  in Fig. 4 and extract the optimal  $f$  factor to be 1. As a measure of the accuracy of extracting that value we take the

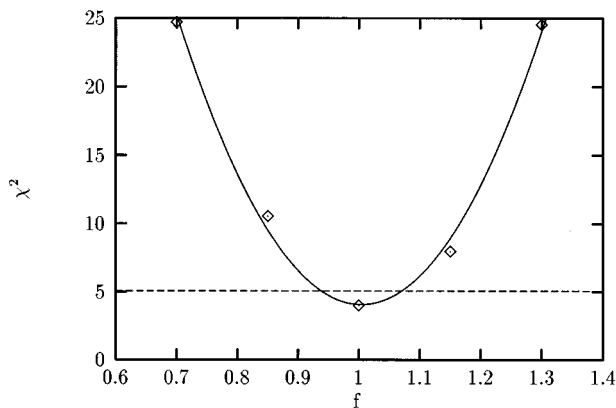


FIG. 4. The  $\chi^2$  from Eq. (83) for  $A_{T'}$  as a function of the strength factor  $f$  from Fig. 3. A parabola is fitted to the calculated values denoted by ( $\diamond$ ). The value  $\chi^2_{\min}+1$  is shown as dashed horizontal line and provides a spread of  $\Delta f = \pm 6.6\%$ .

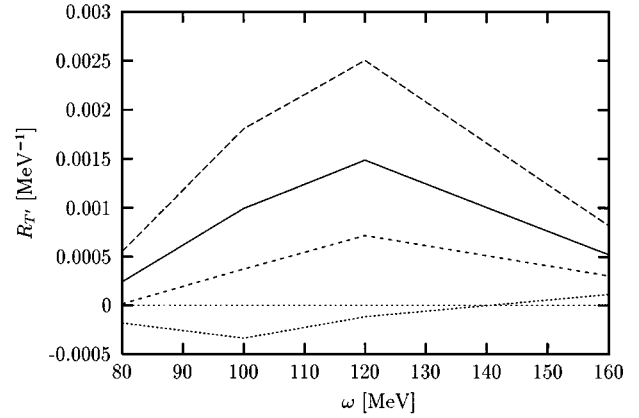


FIG. 5. The transversal structure function  $R_{T'}$  as a function of  $\omega$  in the full calculation for various strength factors  $f$ :  $f=1.3$  (long dashed),  $f=1$  (solid),  $f=0.7$  (short dashed), and  $f=0$  (dotted).

spread in  $f$  for  $\chi^2_{\min}+1$ . This is  $\pm 6.6\%$ . Clearly more precise data would be very welcome to improve on the accuracy of extracting information on  $G_M^{(n)}$ .

The possibly most serious theoretical uncertainty in our analysis is that we do not take MECs into account. Their quantitative contribution remains to be investigated. In a study [22] based on the GFMC method the  $LT'$  and  $TT'$  interference Euclidean response functions of  ${}^3\text{He}$  at  $|\vec{Q}| = 300 \text{ MeV}/c$  have been determined. They show a dependence on two-body currents. Not shown is their effect on the physical responses nor any comparison with data. It also remains to be seen whether different choices of  $NN$  forces could change the results. For inclusive scattering without polarization we found only a very weak dependence [17]. Simplified calculations keeping only  $j_{\max}=1$   $NN$  force components, now for the polarization case, also did not show a dependence on the choice of the  $NN$  force.

For future experimental work we would like to propose to separate  $R_{T'}$  and  $R_{TL'}$ . The sensitivity of  $R_{T'}$  to  $G_M^{(n)}$  is larger than for the asymmetry  $A_{T'}$ . This is demonstrated in Fig. 5 in comparison to Fig. 3 again for the full calculation. Again we quantify that study by evaluating a  $\chi^2$ , defined now as

$$\chi^2(R_{T'}, A_{T'}) \equiv \sum_i \frac{[R_{T'}^{(i)}(A_{T'}^{(i)})(f=1) - R_{T'}^{(i)}(A_{T'}^{(i)})(f=1.3)]^2}{[R_{T'}^{(i)}(A_{T'}^{(i)})(f=1)]^2}, \quad (84)$$

where  $i$  runs over the  $\omega$  values, in which we carried out the calculations. We find  $\chi^2(R_{T'})=3.1$  and  $\chi^2(A_{T'})=2.3$ . Thus  $R_{T'}$  has a stronger dependence on the magnetic neutron form factor (modified by the strength factor  $f$ ) than  $A_{T'}$ . For the sake of curiosity Fig. 5 also includes the results putting  $G_M^{(n)}=0$  ( $f=0$ ).

#### IV. SUMMARY

Inclusive scattering of polarized electrons on polarized  ${}^3\text{He}$  has been evaluated taking the final state interaction fully into account. Realistic  $NN$  forces have been used and the  $3N$

bound state and the  $3N$  continuum are evaluated consistently solving the corresponding Faddeev equations. A formalism proposed in [15], which is ideal for inclusive processes and avoids the tedious direct integration of over all final state configurations, has been generalized to handle new types of structure functions composed of different current components.

The most simple picture of polarized  ${}^3\text{He}$  to be a polarized neutron target fails quantitatively for the energy and momentum transfers considered. That picture relies on the assumption, that the principal  $S$  state is by far dominant. This is not at all true for the transverse-longitudinal asymmetry  $A_{TL'}$ , which receives important contributions from the remaining pieces of the  ${}^3\text{He}$  wave function, but also for the transverse asymmetry  $A_{T'}$ , where the results change significantly when the principal  $S$ -state approximation is replaced by the full and correct  ${}^3\text{He}$  wave function.

We also find that the often used plane-wave impulse approximation (here denoted by PWIA') is insufficient. In PWIA' one takes the  $NN$  force in the final state into account for the pair of nucleons which are spectators to the single nucleon photon absorption of the third nucleon. This is quite insufficient for  $A_{T'}$  and  $A_{TL'}$ . The correct antisymmetrization of the final  $3N$  continuum is important and above all the final state interaction only all three nucleons (full calculation).

In the full calculation the data for  $A_{T'}$  can be described quite well using the Gari-Krümpelmann electromagnetic nucleon form factors. The dependence of that observable  $A_{T'}$  on the neutron  $F_1$  form factor is weak and unimportant. We

optimized the choice of  $G_M^{(n)}$  to the data, with the result that the factor  $f=1$  for the choice of Gari-Krümpelmann parametrization was best. This appears to agree with preliminary results achieved in electron scattering on the deuteron [23].

In the case of  $A_{TL'}$ , the full calculation shows now the enhancement near the  $3N$  breakup threshold, which is present in the data and which was not provided by the plane wave impulse approximation used up to now. For both observables  $A_{T'}$  and  $A_{TL'}$ , more precise data would be very welcome in order to probe the theoretical assumptions more stringently and to extract more accurate information on  $G_M^{(n)}$ .

A more thorough investigation of  $A_{TL'}$ , with respect to the contribution of the proton and the  ${}^3\text{He}$  wave function component is planned. Because of lack of computer time it could not be included in this study.

We would also like to point out that data for  $R_{T'}$  and  $R_{TL'}$  would be more sensitive to electromagnetic nucleon form factors than the asymmetries. From the theoretical point of view mesonic exchange currents should be added and the treatment of relativity remains a pending problem.

#### ACKNOWLEDGMENTS

The authors are indebted to Dr. H. Gao and Dr. C. E. Jones for providing the details of their data. This work was supported by the Science and Technology Cooperation Germany-Poland under Grant No. XO81.91. The numerical calculations were performed on the Cray T90 of the Höchstleistungsrechenzentrum in Jülich, Germany.

#### APPENDIX

We show explicit expression for the four structure functions:

$$\begin{aligned}
R_L &= \mathcal{R}_{\rho\rho 1/2 1/2} = -\frac{3}{\pi} \text{Im} \mathcal{S}_{\rho\rho; 1/2 1/2} \\
&= -\frac{3}{\pi} \text{Im} \left[ \sum_{\mathcal{J}} \frac{1}{E + i\epsilon - p^2/m - (3/4m)q^2} \left\langle pq\alpha \mathcal{J} \frac{1}{2} \left| (1+P)\rho^{(1)} \right| \Psi_{3\text{He}} \frac{1}{2} \right\rangle \left\langle pq\alpha \mathcal{J} \frac{1}{2} \left| U_{\rho} \frac{1}{2} \right\rangle \right], \\
R_T &= \mathcal{R}_{j+1j+1 1/2 1/2} + \mathcal{R}_{j+1j+1 -1/2 -1/2} = -\frac{3}{\pi} \text{Im} (\mathcal{S}_{j+1j+1 1/2 1/2} + \mathcal{S}_{j+1j+1 -1/2 -1/2}) \\
&= -\frac{3}{\pi} \text{Im} \left[ \sum_{\mathcal{J}} \frac{1}{E + i\epsilon - p^2/m - (3/4m)q^2} \left( \left\langle pq\alpha \mathcal{J} \frac{1}{2} \left| (1+P)j_1^{(1)} \right| \Psi_{3\text{He}} - \frac{1}{2} \right\rangle^* \left\langle pq\alpha \mathcal{J} \frac{1}{2} \left| U_{j_1} - \frac{1}{2} \right\rangle \right) \right. \\
&\quad \left. + \left\langle pq\alpha \mathcal{J} \frac{3}{2} \left| (1+P)j_1^{(1)} \right| \Psi_{3\text{He}} \frac{1}{2} \right\rangle^* \left\langle pq\alpha \mathcal{J} \frac{3}{2} \left| U_{j_1} \frac{1}{2} \right\rangle \right) \right]. \tag{A1}
\end{aligned}$$

We see that  $R_L$  and  $R_T$  are independent of the  ${}^3\text{He}$  target polarization:

$$\begin{aligned}
R_{T'} &= \cos \theta^* (\mathcal{R}_{j+1j+1 1/2 1/2} - \mathcal{R}_{j+1j+1 -1/2 -1/2}) = -\frac{3}{\pi} \cos \theta^* \text{Im} (\mathcal{S}_{j+1j+1 1/2 1/2} - \mathcal{S}_{j+1j+1 -1/2 -1/2}) \\
&= \cos \theta^* \frac{3}{\pi} \text{Im} \sum_{\mathcal{J}} \left[ \frac{1}{E + i\epsilon - p^2/m - (3/4m)q^2} \left( \left\langle pq\alpha \mathcal{J} \frac{1}{2} \left| (1+P)j_1^{(1)} \right| \Psi_{3\text{He}} - \frac{1}{2} \right\rangle^* \left\langle pq\alpha \mathcal{J} \frac{1}{2} \left| U_{j_1} - \frac{1}{2} \right\rangle \right) \right. \\
&\quad \left. - \left\langle pq\alpha \mathcal{J} \frac{3}{2} \left| (1+P)j_1^{(1)} \right| \Psi_{3\text{He}} \frac{1}{2} \right\rangle^* \left\langle pq\alpha \mathcal{J} \frac{3}{2} \left| U_{j_1} \frac{1}{2} \right\rangle \right) \right],
\end{aligned}$$

$$\begin{aligned}
R_{TL'} &= -\sin \theta^* \cos \phi^* 2 \operatorname{Re}(\mathcal{R}_{j+1\rho-1/2\ 1/2}) = -\sin \theta^* \cos \phi^* \frac{3}{\pi} \operatorname{Im}(\mathcal{S}_{\rho j+1\ 1/2-1/2}^* - \mathcal{S}_{j+1\rho-1/2\ 1/2}) \\
&= \frac{3}{\pi} \operatorname{Im} \int \left[ \frac{1}{E+i\epsilon-p^2/m-(3/4m)q^2} \left\langle pq\alpha \mathcal{J} \frac{1}{2} \left| (1+P)j_1^{(1)} \right| \Psi_{3\text{He}-\frac{1}{2}} \right\rangle^* \left\langle pq\alpha \mathcal{J} \frac{1}{2} \left| U_{\rho} \frac{1}{2} \right. \right. \right. \\
&\quad \left. \left. - \frac{1}{E-i\epsilon-p^2/m-(3/4m)q^2} \left\langle pq\alpha \mathcal{J} \frac{1}{2} \left| (1+P)\rho^{(1)} \right| \Psi_{3\text{He}\frac{1}{2}} \right\rangle \left\langle pq\alpha \mathcal{J} \frac{1}{2} \left| U_{j_1-\frac{1}{2}} \right. \right. \right] \sin \theta^* \cos \phi^*. \quad (\text{A2})
\end{aligned}$$

- 
- [1] R. G. Arnold *et al.*, Phys. Rev. Lett. **57**, 174 (1986); P. E. Bosted *et al.*, *ibid.* **68**, 3841 (1992).
- [2] P. Markowitz *et al.*, Phys. Rev. C **48**, R5 (1993); J. Jourdan, in *Few-Body Problems in Physics*, Williamsburg, 1994, AIP Conf. Proc. No. 334, edited by F. Gross (AIP, New York, 1994), p. 339; in *Proceedings of the 14th International Conference on Particles and Nuclei*, edited by G. E. Carlson and J. J. Domingo, Williamsburg, 1996 (World Scientific, Singapore, 1997), p. 262.
- [3] B. Blankleider and R. M. Woloshyn, Phys. Rev. C **29**, 538 (1984).
- [4] J. L. Friar, B. F. Gibson, G. L. Payne, A. M. Bernstein, and T. E. Chupp, Phys. Rev. C **42**, 2310 (1990).
- [5] R. Machleidt, Adv. Nucl. Phys. **19**, 189 (1989).
- [6] C. E. Woodward *et al.*, Phys. Rev. Lett. **65**, 698 (1990); C. E. Jones-Woodward *et al.*, Phys. Rev. C **44**, R571 (1991); C. E. Jones *et al.*, *ibid.* **47**, 110 (1993).
- [7] A. K. Thompson *et al.*, Phys. Rev. Lett. **68**, 2901 (1992).
- [8] H. Gao *et al.*, Phys. Rev. C **50**, R546 (1994).
- [9] J.-O. Hansen *et al.*, Phys. Rev. Lett. **74**, 654 (1995).
- [10] C. E. Jones *et al.*, Phys. Rev. C **52**, 1520 (1995).
- [11] R.-W. Schulze and P. U. Sauer, Phys. Rev. C **48**, 38 (1993).
- [12] C. Ciofi degli Atti, E. Pace, and G. Salmé, Phys. Rev. C **51**, 1108 (1995).
- [13] H. Kamada, W. Glöckle, J. Golak, Nuovo Cimento A **105**, 1435 (1992).
- [14] S. Ishikawa, H. Kamada, W. Glöckle, J. Golak, and H. Witała, Nuovo Cimento A **107**, 305 (1994).
- [15] S. Ishikawa, H. Kamada, W. Glöckle, J. Golak, and H. Witała, Phys. Lett. B **339**, 293 (1994).
- [16] J. Golak, H. Kamada, H. Witała, W. Glöckle, and S. Ishikawa, Phys. Rev. C **51**, 1638 (1995).
- [17] J. Golak, H. Witała, H. Kamada, D. Hüber, S. Ishikawa, and W. Glöckle, Phys. Rev. C **52**, 1216 (1995).
- [18] T. W. Donnelly and A. S. Raskin, Ann. Phys. (N.Y.) **169**, 247 (1986).
- [19] M. E. Rose, *Elementary Theory of Angular Momentum* (Wiley, New York, 1957).
- [20] W. Glöckle, *The Quantum Mechanical Few-Body Problem* (Springer-Verlag, Berlin, 1983).
- [21] M. Gari and W. Krümpelmann, Phys. Lett. B **173**, 10 (1986).
- [22] R. Schiavilla, in *Workshop on Electron-Nucleus Scattering*, edited by O. Benhar and A. Fabrocini (Edizioni ETS, 1996), p. 237.
- [23] J. Jourdan (private communication).